New Radiative Recombination Processes Involving Neutral Donors and Acceptors in Silicon and Germanium

P. J. DEAN,* J. R. HAYNES,† AND W. F. FLOOD

Bell Telephone Laboratories, Murray Hill, New Jersey

(Received 10 April 1967)

Relatively weak extrinsic luminescence bands observed at low temperatures ($\lesssim 80°$K) in silicon doped with several different donors and acceptors are described and identified with the following recombination processes: (1) Phonon-assisted decay of excitons bound to neutral centers involving the momentum-conserving (MC) transverse acoustical phonon; also multiphonon transitions involving the zone-center optical phonon together with the MC transverse optical phonon. The phonon energies and relative intensities of these replicas are shown to be very similar to those observed in the intrinsic luminescence bands in silicon. The relationship between the relative strength of the no-phonon band and the impurity ionization energy is discussed. (2) "Two-electron" transitions, in which an exciton bound to a neutral impurity center decays, leaving the impurity center in a bound excited state. (3) "Two-electron" transitions, observed only for donor centers, in which a free exciton in the vicinity of a neutral donor center decays, leaving the donor in an excited valley-orbit state. (4) Radiative recombination of a free hole (or electron) with the second electron (or hole) in a newly observed H⁻-like complex involving the shallow donor and acceptor centers. (5) Radiative recombination of a free electron with a neutral acceptor center, observed only for the relatively deep acceptors gallium and indium. Processes (1) and (3) are significant only below ~50°K, while transitions (4) and (5) are observed only above ~30°K. Process (3) is significant at all temperatures investigated. Unidentified lines reported by Benoit à la Guillaume and Parodi in the low-temperature edge luminescence of doped germanium are shown to be consistent with mechanisms (2) and (3), while other lines previously discussed by them in terms of mechanism (5) are in closer agreement with mechanism (4). These "two-electron" transitions in silicon and germanium all appear to contain donor or acceptor excitations involving no parity change, in contrast to similar transitions in gallium phosphide. The ionization energies of the H⁻-like complexes in silicon and germanium are ~4 meV and ~1.5 meV, respectively.

I. INTRODUCTION

SILICON is well known as an indirect band-gap semiconductor in which the lowest-energy interband transitions occur between the degenerate valence-band maximum at the center of the reduced zone (symmetry $\Gamma_{25'}$) and six equivalent conduction-band minima on $\langle 100 \rangle$-type axes of the reduced zone (symmetry Δ_1).[1] The exact positions of these minima were found experimentally from the *intrinsic* interband absorption[2] and luminescence[3] spectra of silicon by measurement of the energies of the momentum-conserving (MC) phonons selected in the interband transitions and a comparison of these energies with the lattice dispersion curves of silicon, which had been measured by inelastic neutron scattering.[4]

Extrinsic components were also observed in the luminescence spectra of silicon crystals doped with neutral shallow donor and acceptor centers, and the presence of no-phonon as well as MC transverse-optical (TO) phonon-assisted components has been briefly reported.[5] The present paper is concerned with a more detailed study of the low-temperature luminescence

from silicon containing neutral donor and acceptor centers. Partially radiative "two-electron" recombination processes, in which an interbound state transition of a donor electron or acceptor hole is induced during the recombination of both bound and free excitons, have been identified in the luminescence spectra from doped silicon. The "two-electron" luminescence process has previously been recognized (in gallium phosphide) only in the recombination of bound exciton states.[6] Additional luminescence bands, observed only at temperatures $\gtrsim 30°$K, are interpreted as arising from the recombination of a free hole (or electron) with H⁻-like states consisting of a neutral donor which has trapped a second electron (or neutral acceptor which has trapped a second hole). The theoretical stability of these H⁻-like donor or acceptor complexes in semiconductors was pointed out by Lampert in 1958,[7] but the present work provides the first experimental evidence for their existence. The application of these new ideas to the interpretation of the detailed structure in the extrinsic luminescence of germanium is briefly discussed in the final section of the paper.

II. EXPERIMENTAL

The luminescence of excitons weakly bound to neutral donors is of roughly comparable magnitude to the luminescence of free excitons or of excitons bound to neutral acceptors in silicon, and is very inefficient.[8]

* On leave of absence from Wheatstone Laboratory, King's College, Strand, London WC2, England.
† Deceased.
[1] B. Lax, Rev. Mod. Phys. **30**, 122 (1958).
[2] T. P. McLean, *Progress in Semiconductors* (Heywood and Company, Ltd., London, 1960), Vol. 5, p. 53.
[3] J. R. Haynes, M. Lax, and W. F. Flood, Phys. Chem. Solids **8**, 392 (1959); in *Proceedings of the International Conference on the Physics of Semiconductors, Prague, 1960* (Academic Press Inc., New York, 1960), p. 423.
[4] B. N. Brockhouse, Phys. Rev. Letters **2**, 256 (1959).
[5] J. R. Haynes, Phys. Rev. Letters **4**, 361 (1960).

[6] P. J. Dean, J. D. Cuthbert, D. G. Thomas, and R. T. Lynch, Phys. Rev. Letters **18**, 122 (1967).
[7] M. A. Lampert, Phys. Rev. Letters **1**, 450 (1958).
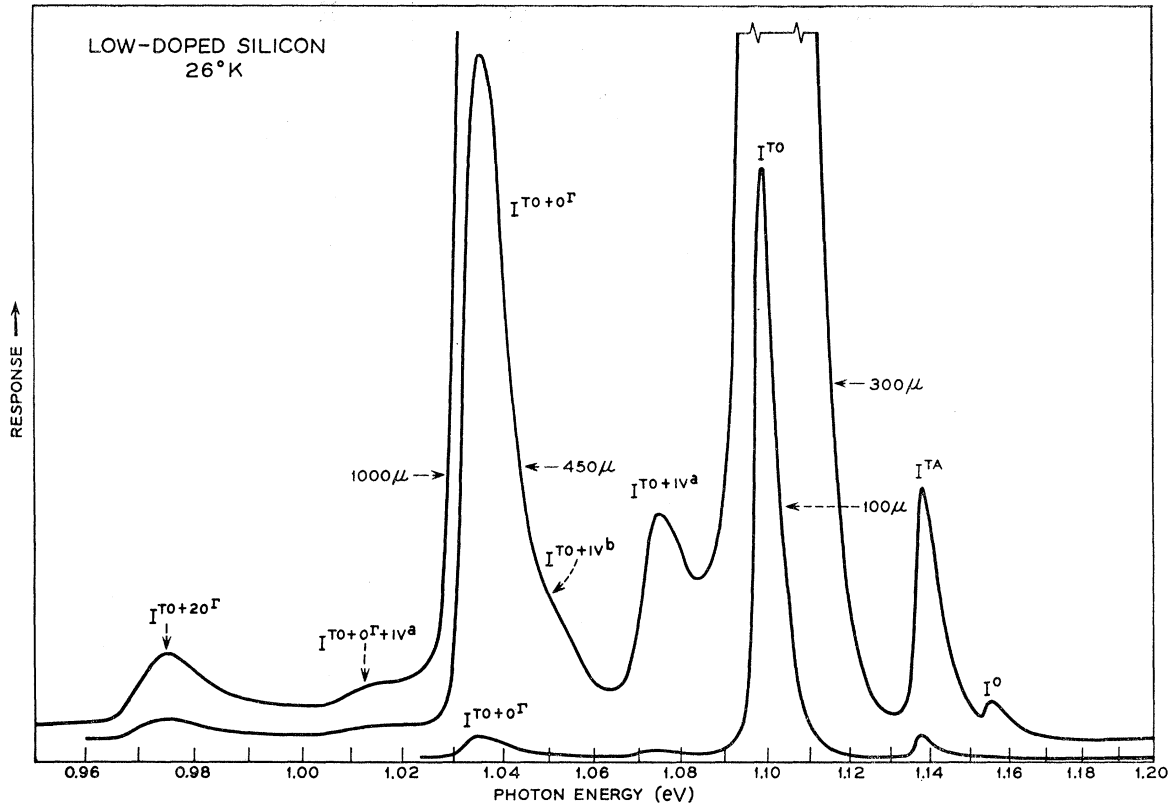[8] D. F. Nelson, J. D. Cuthbert, P. J. Dean, and D. G. Thomas, Phys. Rev. Letters **17**, 1262 (1966).

FIG. 1. Low-temperature photoluminescence spectra from a silicon crystal containing 2×10^{14} cm^{-3} phosphorus atoms. All the bands shown, excepting I^0, are intrinsic and due to the recombination in the pure lattice of free excitons assisted by the indicated phonons. The no-phonon component I^0 is forbidden for pure silicon, and is discussed in the text. The high-gain spectra were obtained at the expense of spectral resolution. The ordinate is nearly proportional to the number of photons per unit energy interval.

The luminescence associated with these transitions falls in the energy interval $\sim 1.0 \rightarrow 1.2$ eV, just outside the usefully sensitive range of photomultiplier detectors. It is therefore necessary to use carefully designed optical systems of wide aperture[9] for the excitation and detection of the photoluminescence of silicon if spectra of high energy-resolution are desired.

High concentrations of excess electrons and holes were produced by focusing light from a 200-W mercury arc onto an etched surface of the specimen. The mercury light was filtered by a 1-cm water cell with windows consisting of two 0.5-cm-thick Jena KG1 filters. The luminescence was detected from the irradiated surface in some measurements and from the opposite surface in others. The specimen thickness was generally ~ 1 mm. The luminescence was analyzed with a Perkin-Elmer Model 112 spectrometer, equipped with a Bausch and Lomb 600 line/mm grating and a cooled lead-sulphide photodetector. Optimum sensitivity was obtained by chopping the incident light at 25 cps and using conventional lock-in techniques to detect and amplify the signal from the photocell.

The photoluminescence efficiency was found to be very sensitive to the condition of the surface of the silicon crystals for the relatively nonpenetrating excitation used in this work. At a typical excitation energy of ~ 2.5 eV, the absorption coefficient is $\sim 10^4$ cm^{-1}.[2] A generally successful empirical procedure was evolved whereby the etched surfaces were steamed for ~ 20 min immediately before the sample was mounted in the Dewar.

No radiation was detected from many of the doped crystals examined because the free-carrier lifetimes were too low. It was generally advantageous to use samples cut close to the seed end of boules grown by the Czochralski technique. Efficient luminescence was generally difficult to obtain from silicon doped with the relatively insoluble impurities like indium or bismuth except at concentrations $\lesssim 10\%$ of those used for soluble impurities like boron or phosphorus, so that extrinsic components were relatively weak for the former impurities.

In the early work, the specimens were mounted in the vacuum space of a conventional cold finger-type Dewar, using silver-loaded silicone grease to ensure good thermal contact to the crystal. Temperatures below $25 \rightarrow 30$°K were unattainable with this arrangement,

[9] J. R. Haynes, in *Methods of Experimental Physics*, edited by K. Lark Horovitz and V. A. Johnson (Academic Press Inc., New York, 1959), Vol. 6, Part B, p. 322.

even when liquid helium or pumped liquid hydrogen was used in the Dewar, because of the differential heating of the specimen relative to the copper block under the ~7-W excitation power necessary for these experiments. The later low-temperature spectra were therefore obtained with the specimen directly immersed in the liquid refrigerant. Analysis of the Maxwell-Boltzmann (M.B.) intensity profiles of the intrinsic luminescence bands due to the recombination of free excitons indicated that the lattice temperature in the excited region of the crystal was close to the refrigerant temperature over the useful temperature range (15 → 20.6°K) of pumped liquid hydrogen. This was not true for liquid helium below the λ point.[10] Few spectra were taken at helium temperatures in the present work, however, because much of the spectral region of interest was obscured by the broad bands due to the recombination of the free excitonic molecule.[10] These excitonic molecule bands are prominent under high excitation densities at ~3°K even in specimens containing ~10^{17} cm^{-3} donor or acceptor centers.

III. RESULTS

A. Intrinsic Material

Relatively weak extrinsic luminescence bands connected with the presence of donor or acceptor centers were of interest in the present work. It was therefore essential to clearly recognize all the spectral features associated with recombination of free excitons. These are shown in Fig. 1. Four components are resolved in the high-resolution spectrum as previously reported.[3] Two more become visible at lower energies in the increased signal obtained at lower spectral resolving power, and an additional weak component can be seen superimposed on the high-energy tail of the TO(MC) +O$^\Gamma$ component near 1.05 eV. The spectrometer slit-width setting (in microns) is shown for each spectrum in Fig. 1 and in the subsequent spectra from doped silicon (Figs. 2–11). The relevant spectral resolution may be judged from the latter spectra using the half-height bandwidths of the principal bound exciton (BE) components BE^O and BE^{TO}, which were invariably determined by the instrumental resolution in these measurements.

The threshold energies of these free-exciton luminescence bands are listed and analyzed in Table I. Only transverse phonons are observed in the one-phonon-assisted components,[3] and their energies are consistent with the most recent previous estimates.[2,5] These phonons conserve electron momentum in the indirect interband transition.

The two weak components near 1.05 and 1.075 eV have been attributed to recombinations during which the electron is scattered between the six equivalent conduction-band valleys.[11] Group theory shows that

[10] J. R. Haynes, Phys. Rev. Letters **17**, 860 (1966).
[11] W. P. Dumke, Phys. Rev. **118**, 938 (1960).

TABLE I. Analysis of intrinsic recombination radiation bands from silicon at 26°K.[a,b]

Threshold energy (eV)	Phonon energy (meV)	Analysis	Assignment	Relative intensity
1.1545	~0	No-phonon	NP	~0.004
1.1365	18.3	18.3	TA(MC)	0.035
1.0970	57.8	57.8	TO(MC)	1.00
1.074	80.8	57.8+23	TO(MC)+IV^a	0.016
1.051	103.8	57.8+46	TO(MC)+IV^b	~0.008
1.0315	122.3	57.8+64.5	TO(MC)+O$^\Gamma$	0.07
1.013	142	57.8+64.5+21.5	TO(MC)+O$^\Gamma$+IV^a	~0.0025
0.968	187	58+64.5+64.5	TO(MC)+2O$^\Gamma$	~0.01

[a] The threshold energies were determined by fitting against Maxwell-Boltzmann (M.B.) intensity distributions. An empirical procedure was used for the broader multiphonon assisted components, with an allowance for the effect of instrumental resolution. The peak energies were used for the analysis of the intervalley (IV) components, since the low-energy tail is then largely determined by the energy-wave-vector dependence of the LA phonon. The exciton energy gap E_{gx} was assumed to be 1.1548 eV at 26°K.

[b] *Notation:* TA—transverse acoustical, TO—transverse optical, LA—longitudinal acoustical, Γ—center of reduced zone–zero wave vector, MC—momentum conserving phonon, IV—phonon selected for intervalley scattering of electron (two phonons, a and b).

intervalley scattering is allowed for longitudinal acoustical phonons.[12] Dumke has calculated that the conduction-band minima in silicon are at (0.82,0,0)-type positions in the reduced zone, assuming that the 23 meV intervalley phonon IV^a is selected for scattering between valleys on the same axes.[11]

Table I shows that the low-energy threshold of the weak component labeled I^0 in Fig. 1, which also has an M.B. intensity profile consistent with the radiative recombination of free excitons, is close to the exciton energy gap E_{gx}. This band therefore apparently arises from the no-phonon (NP) recombination of free indirect excitons, a process which is forbidden in a perfect crystal of silicon. The intensity ratio NP/TO(MC) is small (~0.4%). Well-defined M.B. components of similar transition energy and relative intensity have occasionally been observed in the low-temperature luminescence spectra of n-type doped crystals in which the bound exciton components are prominent. It is therefore unlikely that these forbidden transitions are connected with the presence of shallow donor centers, but must involve other defect or impurity centers.[13]

Table I also shows that the relatively weak components below 1.05 eV in Fig. 1 have low-energy thresholds consistent with processes involving the multiple emission of zone center (O$^\Gamma$) phonons. Similar components have been observed in the intrinsic exciton luminescence of diamond.[14]

[12] M. Lax, in *Proceedings of the International Conference on Semiconductor Physics, Exeter, 1962* (The Institute of Physics and The Physical Society, London, 1962), p. 395.
[13] It has recently been shown that the band I^0 is analogous to an absorption component, with low-energy threshold at E_{gx}, recently identified in arsenic-doped gallium phosphide with the creation of free excitons in the vicinity of the arsenic centers. Arsenic substituting for phosphorus produces weak isoelectronic scattering centers in gallium phosphide. The relevant isoelectronic center in silicon is substitutional carbon which, unlike nitrogen in gallium phosphide, does not produce bound-exciton states.
[14] P. J. Dean, E. C. Lightowlers, and D. R. Wight, Phys. Rev. **140**, A352 (1965).
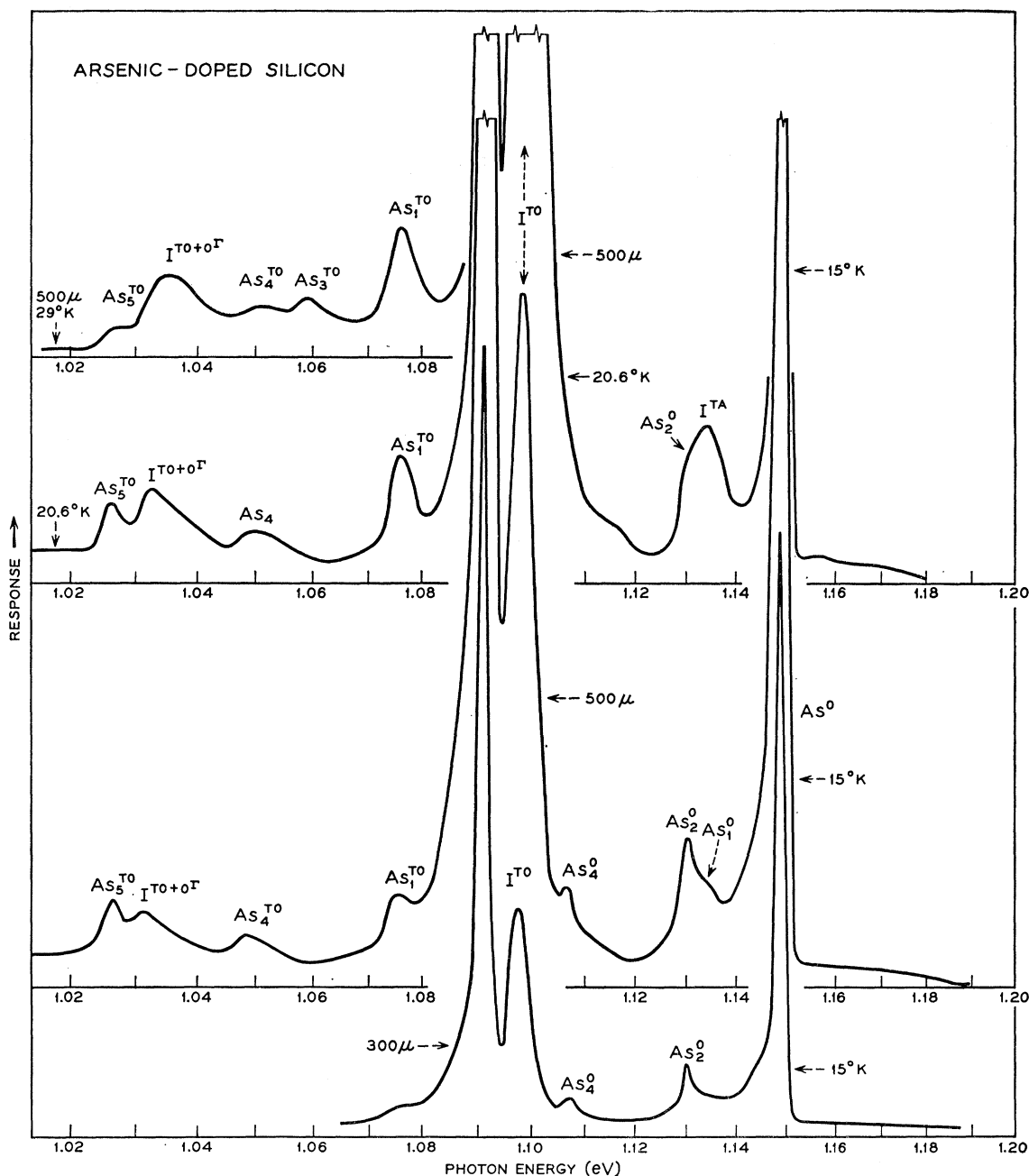
FIG. 2. Low-temperature photoluminescence spectra from a silicon crystal containing 2×10^{17} cm^{-3} arsenic atoms. Components As are extrinsic, components I are intrinsic. The notation is discussed in the text. The ordinate is nearly proportional to the number of photons per unit energy interval.

B. Doped-Material: Luminescence Associated with Neutral Donors

(1) Arsenic

Detailed photoluminescence spectra obtained at four different temperatures from a crystal containing 2×10^{17} cm^{-3} arsenic donor centers are shown in Figs. 2 and 3. The 15°K spectrum is dominated by two

sharp lines at $\sim$1.149 and $\sim$1.091 eV, which are, respectively, due to the no-phonon and TO(MC)-phonon-assisted decay of excitons bound to neutral donor centers.[5] Additional extrinsic components are clearly evident in the high-gain spectra of Fig. 2. These components are listed in Table II, where it is shown that, like the principal 1.149- and 1.091-eV components, the weaker components can be arranged in pairs corre-

TABLE II. Extrinsic recombination radiation bands from silicon associated with neutral donor centers.[a]

Donor and component	Transition energy (eV)	Energy relative to $BE^0(a)$, $E_{gx}(b)$, $E_g(c)$ (meV)		Energy relative to $BE^{TO}(a)$, $E_{gx}^{TO}(b)$, $E_g^{TO}(c)$ (meV)		Relative intensity
Arsenic As^0	1.1488 (15°K)	(a)	0			0.8
Arsenic As_1^0	1.132 (15°K)	(b)	~23			
Arsenic As_2^0	1.1303 (15°K)	(a)	18.5			0.05
Arsenic As_3^0	1.1155 (20.6°K)	(c)	~47.5			
Arsenic As_4^0	1.1068 (20.6°K)	(a)	42			0.015
Arsenic As^{TO}	1.0907 (15°K)	(a)	58.1			1.00
Arsenic As_1^{TO}	1.075 (20.6°K)			(b)	22.3	
Arsenic As_3^{TO}	1.0573 (28°K)			(c)	47.5	
Arsenic As_4^{TO}	1.0482 (20.6°K)			(a)	42.5	
Arsenic As_5^{TO}	1.0262 (15°K)			(a)	64.5	0.02
Phosphorus P^0	1.1496 (15°K)	(a)	0			0.35
Phosphorus P_1^0	1.1415 (15°K)	(b)	13.4			
Phosphorus P_2^0	1.1311 (15°K)	(a)	18.5			0.06
Phosphorus P_4^0	1.116 (15°K)	(a)	~34			~0.02
Phosphorus P_6^0	1.1231 (15°K)	(b)	31.8			
Phosphorus P^{TO}	1.0916 (15°K)	(a)	58.0			1.00
Phosphorus P_1^{TO}	1.0838 (15°K)			(b)	13.5	
Phosphorus P_3^{TO}	1.0663 (30°K)			(c)	38.5	
Phosphorus P_4^{TO}	1.0580 (15°K)			(a)	33.6	
Phosphorus P_5^{TO}	1.0271 (15°K)			(a)	64.5	0.02
Antimony Sb^0	1.1501 (15°K)	(a)	0			0.03
Antomony Sb_2^0	1.1318 (15°K)	(a)	18.3			0.05
Antimony Sb_4^0	1.119 (15°K)	(a)	31			
Antimony Sb_6^0	1.1245 (15°K)	(b)	~31			
Antimony Sb^{TO}	1.0921 (15°K)	(a)	58.0			1.00
Antimony Sb_1^{TO}	1.0852 (15°K)			(b)	12.1	
Antimony Sb_3^{TO}	1.068 (64°K)			(c)	~36	
Antimony Sb_4^{TO}	1.0615 (15°K)			(a)	~31	~0.10
Antimony Sb_5^{TO}	1.0277 (15°K)			(a)	64.4	0.02
Bismuth Bi^0	1.1469 (15°K)	(a)	0			2.2
Bismuth Bi_2^0	1.1288 (15°K)	(a)	18.1			0.08
Bismuth Bi^{TO}	1.0888 (15°K)	(a)	58.1			1.00
Bismuth Bi_5^{TO}	1.0242 (27°K)			(a)	64.2	~0.025

[a] The following values of the exciton energy gap were assumed: 1.1553 eV (15 and 20.6°K); 1.1548 eV (~30°K); 1.1533 eV (64°K). The exciton ionization energy E_x was assumed to be 8 meV. Index TO denotes that the transition involves the emission of a TO(MC) phonon. Index 0 denotes other transitions. The subscripts indicate components having different transition mechanisms as discussed in the text.

sponding to no-phonon transitions or transitions in which a TO(MC) phonon is emitted. Only the TO(MC) members of the pairs of components can be clearly seen at the high temperatures (Fig. 3). The notation used in Fig. 2, in subsequent figures, and in Table II is summarized in Sec. VI together with the interpretations discussed in Secs. IV and V.

The relative energy of each of the components listed in columns 3 and 4 of Table II has been determined from one of three different energy positions as indicated. The relative intensities of components As_2^0, (As_4^0, As_4^{TO}), As_5^{TO}, and (As^0, As^{TO}) were found to be constant. The bound exciton complexes responsible for (As^0, As^{TO}) undergo thermal dissociation at the higher temperatures[5] leaving the intrinsic components I^{TO}, etc., predominant (Fig. 3). The energies of As_2^0, As_4^0 and As_4^{TO}, As_5^{TO} were therefore measured relative to As^0 and As^{TO}. The association of components (As_1^0, As_1^{TO}) and (As_3^0, As_3^{TO}), respectively, with the reference energies (E_{gx}, E_{gx}^{TO}) and (E_g, E_g^{TO}) is less straightforward, and depends upon a detailed consideration of the origin of the different displacement energies as given in Sec. IV. The association of As_1^{TO} with E_{gx}^{TO} is supported by the experimental observation that the intensities of components As_1^{TO} and I^{TO} are related and increase together relative to the bound exciton component As^{TO} between 15 and 20.6°K.

Figure 3 shows that only extrinsic components As_1^{TO} and As_3^{TO} are observed at 64°K. Component As_3^{TO} has an M.B. intensity profile, consistent with radiative recombination within a system containing one free particle.[3] Component As_1^{TO} rises more steeply from threshold than the M.B. function at 63°K, and occurs as a relatively sharp line compared with the intrinsic components at lower temperatures (e.g., the 20.6°K spectrum in Fig. 2). The peak of As_1^{TO} in Fig. 3 is ~23 meV below that of I^{TO}, and the estimated low-energy threshold of As_3^{TO} (1.057 eV) is ~48 meV
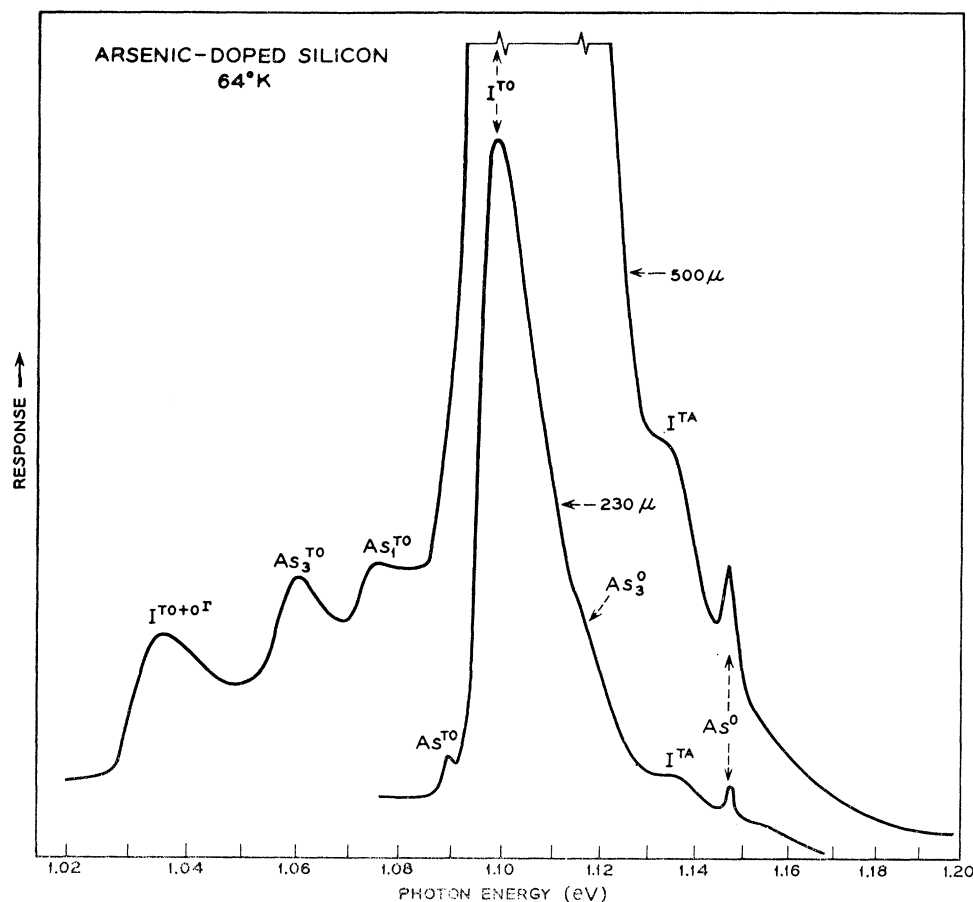
FIG. 3. Higher-temperature photoluminescence spectra from a silicon crystal containing 2×10^{17} cm^{-3} arsenic atoms. The extrinsic components As$_1^{TO}$ and As$_3^{TO}$ involve the recombination of free particles at neutral arsenic donors (see text). Residual components As^0 and As^{TO} involve the decay of excitions bound to neutral arsenic donors. The ordinate is nearly proportional to the number of photons per unit energy interval.

below E_g^{TO}. These energies are consistent with the low-temperature results of Fig. 2 analyzed in Table II. It should be particularly noticed that As$_3^{TO}$ is not observed at 15°K, but grows rapidly relative to the intrinsic components with increasing temperature above ~25°K.

(2) Phosphorus

The luminescence components associated with the presence of phosphorus donors (Fig. 4) have been labeled in accordance with the notation used in Fig. 2, and the energies are listed in Table II. The most striking differences between the arsenic and phosphorus spectra are:

(a) The intensity ratio of the principal bound exciton no-phonon and TO(MC)-phonon-assisted components is appreciably less for phosphorus.

(b) The intensity ratios P_1^0/P^0 and P_1^{TO}/P^{TO} are much larger than the corresponding arsenic value at the same temperature; moreover, the energy interval $P^0 \rightarrow P_1^0$ is much less than As$^0 \rightarrow$ As$_1^0$. This means that the O$^\Gamma$ replica of component P_1^{TO} can be readily seen (Fig. 4). The P_1^0 no-phonon line is significantly stronger relative to P_1^{TO} (~60%) than the corresponding ratio exhibited by the P^0 and P^{TO} bound exciton

components (~35%), although the lower-energy P_4^0 and P_4^{TO} components, as well as the corresponding arsenic components, exhibit ratios very similar to the principal bound exciton components. This difference supports the view that the $(_4^0)$, $(_4^{TO})$ components are bound exciton satellites (Sec. IV B), whereas the $(_1^0)$, $(_1^{TO})$ components are not (Sec. IV C).

Comparison of Figs. 2–4 shows that the intensities of corresponding luminescence components in the arsenic and phosphorus spectra behave similarly with increasing temperature. Component P_4^{TO} is only observed at the lower temperatures like the principal BE component P^{TO}, while P_3^{TO} appears only at higher temperatures and P_1^{TO} can be seen at all temperatures between 15 and 80°K.

(3) Antimony

The extrinsic components in the low-temperature luminescence spectrum of antimony-doped silicon (Fig. 5) are more like those associated with phosphorus than with arsenic, in particular the energy interval I^{TO}–Sb$_1^{TO}$ is relatively small (Table II). Component Sb$_1^{TO}$ is relatively strong compared with Sb^{TO} at 15°K, although Sb$_1^0$ is not visible and Sb^0 is relatively weak.
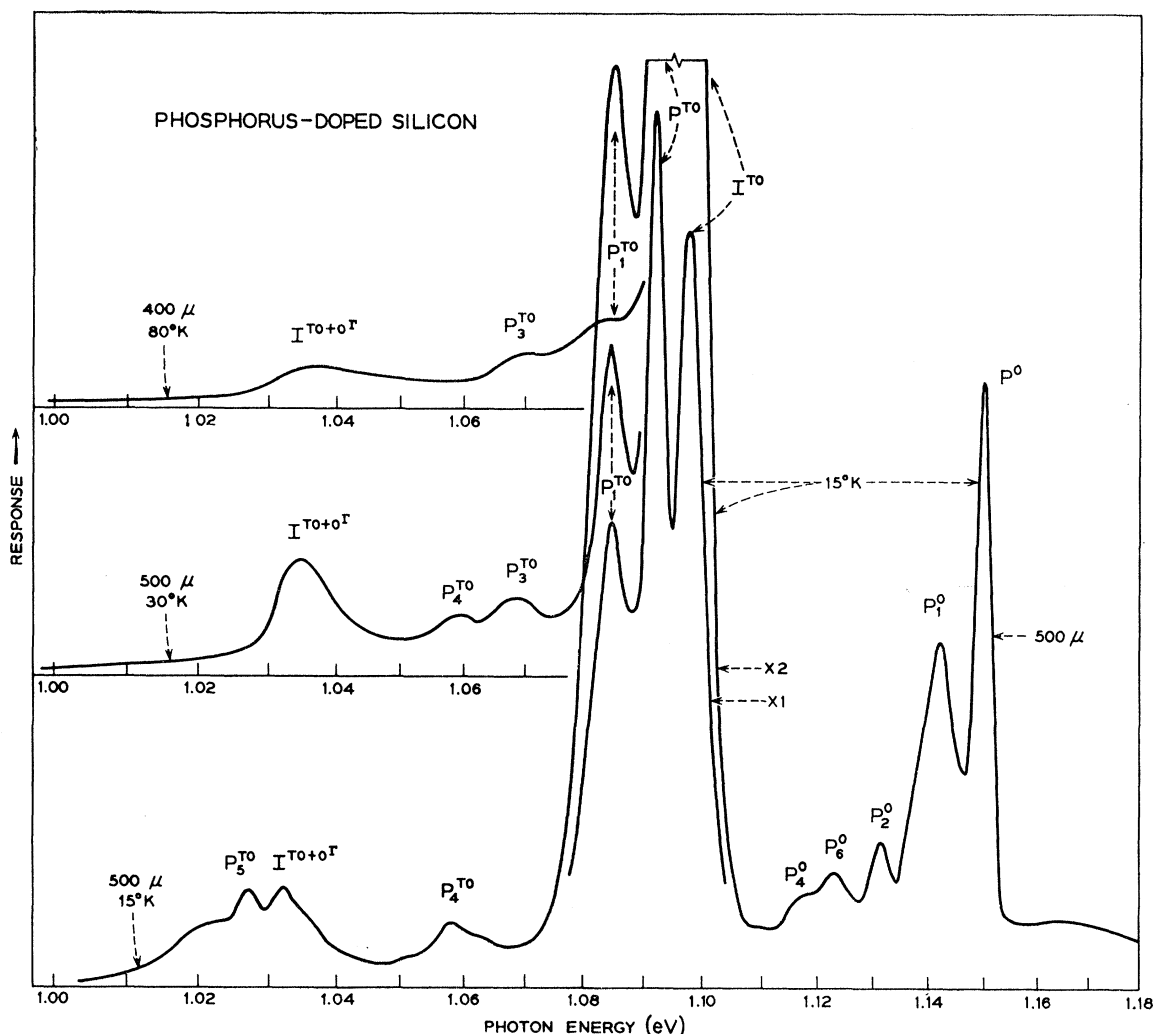
FIG. 4. Photoluminescence spectra from a silicon crystal containing 8×10^{16} cm^{-3} phosphorus atoms (cf. Fig. 1). Components P are extrinsic, components I are intrinsic. The notation is consistent with Figs. 2 and 3, and is discussed in the text. The ordinate is nearly proportional to the number of photons per unit energy interval. Symbols "$X1$" and "$X2$" denote the relative ordinate amplification factor at constant spectral resolution.

Figures 4 and 5 show even more clearly than Fig. 2 the narrow profile of the ($_1^{TO}$) components compared with the intrinsic components at intermediate low temperatures. Component Sb_1^{TO} is broader at 15°K than at 21°K, apparently because of additional underlying transitions present at the lower temperature, since the peak of Sb_1^{TO} remains narrow at 15°K (see Sec. IV C).

Only the extrinsic components Sb_1^{TO} and Sb_3^{TO} were observed at 64°K (Fig. 6), in agreement with the results for arsenic and phosphorus-doped silicon shown in Figs. 3 and 4.

(4) Bismuth

The luminescence from the relatively lightly bismuth-doped crystal was weak at 15°K, and Fig. 7 shows that fewer extrinsic components were detected. Unlike the other donors, the intensity ratio Bi^0/Bi^{TO} is >1 (Table II). The fact that components Bi_1^0 and Bi_1^{TO} are not observed in Fig. 7 is consistent with the trend noted in Figs. 2, 4, and 5 that the low-temperature intensities of these components relative to the principal BE lines decrease rapidly with increase in their displacement energy.

C. Doped Material: Luminescence Associated with Neutral Acceptors

(1) Boron

The photoluminescence spectra from boron-doped silicon (Fig. 8) contain fewer extrinsic components than the donor spectra discussed above. The notation in Fig. 8 conforms with that used in the donor spectra of Figs. 2–7 in that components associated with the same type of transition have the same subscript and
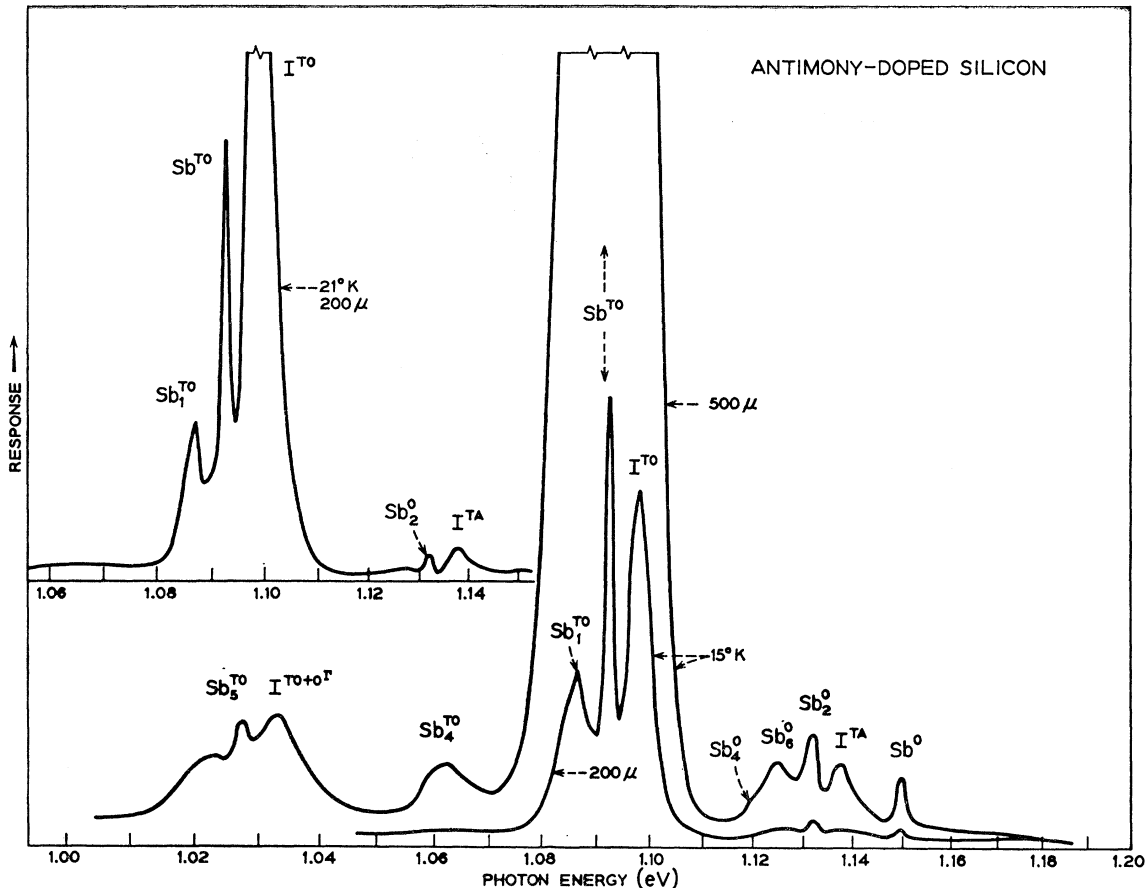
FIG. 5. Low-temperature photoluminescence spectra from a silicon crystal containing 9×10^{16} cm^{-3} antimony atoms. Components Sb are extrinsic, components I are intrinsic. The notation is consistent with Figs. 2 and 3, and is discussed in the text. The ordinate is nearly proportional to the number of photons per unit energy interval.

superscript, assuming that holes and electrons may be regarded as interchangeable particles for this purpose. It should be particularly noted that components with subscript 1 do not appear in the acceptor spectra (see Sec. IV C).

Consistent with the behavior of the corresponding donor components, Fig. 8 shows that $B_3{}^{TO}$ increases in relative intensity with increasing temperature, while the reverse is true for $B_4{}^{TO}$. Component $B_4{}^{TO}$ is narrower than in the low-temperature donor spectra. The corresponding no-phonon satellite components $B_3{}^0$ and $B_4{}^0$ were not observed, and the principal no-phonon BE component B^0 is very weak.

The position of component $B_3{}^{TO}$ at 64°K (Fig. 8) is consistent with the 30°K data given in Table III, allowing for the $\sim$1.5-meV decrease in E_g between 30 and 64°K, and also for the increasing width of the Maxwell-Boltzmann profile of $B_3{}^{TO}$ with temperature.

A weak tail can be seen on the low-energy side of component B^{TO} in Fig. 8. Similar asymmetric line shapes have been observed in the principal BE transitions involving neutral donors (e.g., Fig. 2). This asym-

metry is due to acoustical-phonon-assisted transitions.[15] Significant coupling occurs only to phonons of very low energy (long wavelength) because of the large spatial extent of indirect exciton states in silicon.[16]

(2) Gallium

Component $Ga_4{}^{TO}$ would be predicted to lie $\sim$62 meV below Ga^{TO} (Sec. IV B) and is therefore obscured by $Ga_5{}^{TO}$ in the 30°K spectrum shown in Fig. 9. Component $Ga_3{}^{TO}$ is very prominent compared with the main intrinsic component I^{TO} in both the 30 and 80°K spectra. The intensity ratio of $Ga_3{}^{TO}$ and Ga^{TO} varies considerably between these temperatures, supporting the view that $Ga_3{}^{TO}$ is not a BE satellite (Table III). The luminescence from this crystal was weak and successful low-temperature spectra were not obtained with the crystal immersed in liquid refrigerant.

---

[15] J. J. Hopfield, in *Proceedings of the International Conference on Semiconductor Physics, Exeter, 1962* (The Institute of Physics and The Physical Society, London, 1962), p. 75.

[16] Effective-mass calculations indicate that the free exciton has a diameter of $\sim$120 Å if E_x is 8 meV (Ref. 3).

(3) Indium

The intensity ratio of the principal BE components In^0 and In^{TO} (Fig. 10) is much larger than for the donors or acceptors discussed so far. The luminescence from this relatively lightly doped crystal was weak, and exceptionally large spectral slit widths were used for Fig. 10. The only identifiable extrinsic satellite components are In_3^0 and In_3^{TO}. These components were more prominent at 100°K than at 30°K, and In_3^{TO} was superimposed upon a broad featureless luminescence band which extended to $\lesssim 0.9$ eV. Only the high-energy portion of this band, which has a high-energy threshold near In_3^0, is shown in Fig. 10.

There are also in Fig. 10 two broad bands above E_{gx} (~ 1.155 eV at 30°K). These bands are particularly strong in the indium spectra, but the lower-energy band, which appears to have a low-energy threshold near E_{gx}, is also clearly visible in the luminescence spectra of gallium-doped silicon (Fig. 9). These bands were observed in the absence of a silicon sample, and
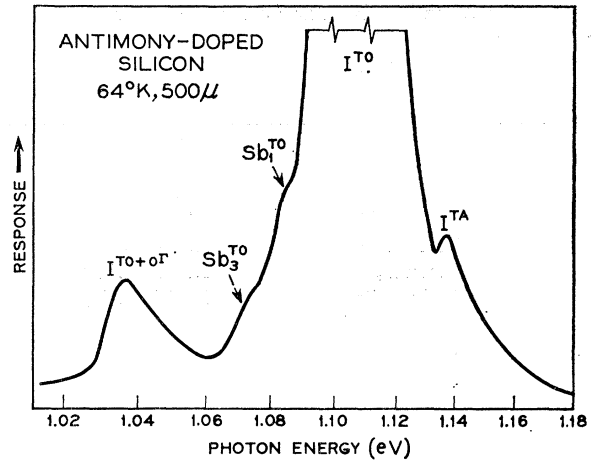

FIG. 6. Higher-temperature photoluminescence spectrum of a silicon crystal containing 9×10^{16} cm^{-3} antimony atoms. Extrinsic components Sb_1^{TO} and Sb_3^{TO} involve the recombination of free particles at neutral antimony donors (see Fig. 3, and text). The ordinate is nearly proportional to the number of photons per unit energy interval.
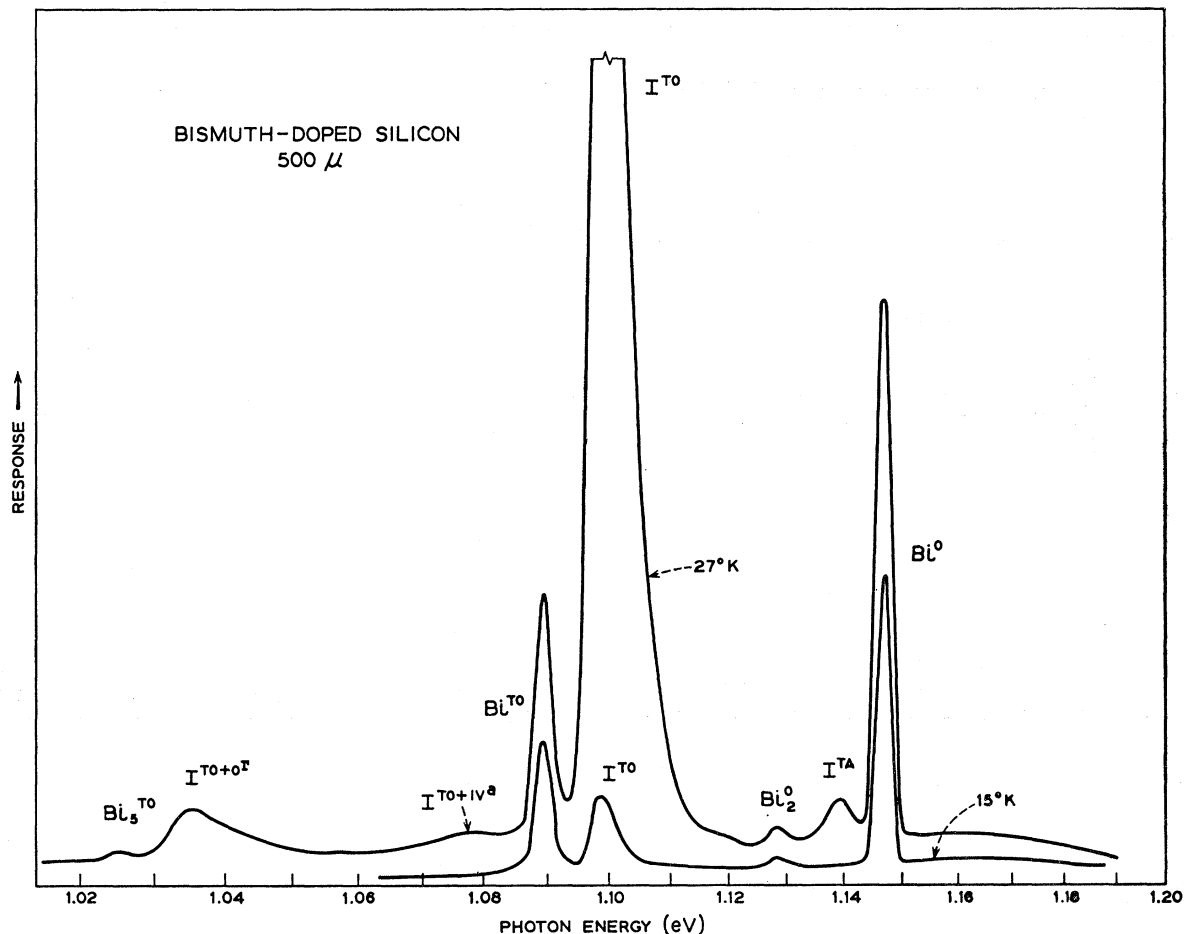

FIG. 7. Low-temperature photoluminescence spectra of a silicon crystal containing 3×10^{16} cm^{-3} bismuth atoms. Components Bi are extrinsic, components I are intrinsic. The notation is consistent with Figs. 2 and 3, and is discussed in the text. The ordinate is nearly proportional to the number of photons per unit energy interval.

TABLE III. Extrinsic recombination radiation bands from silicon associated with neutral acceptor centers.[a]

Acceptor and component	Transition energy (eV)	Energy relative to $BE^0(a)$, $E_{gx}(b)$, $E_g(c)$		Energy relative to $BE^{TO}(a)$, $E_{gx}^{TO}(b)$, $E_g^{TO}(c)$		Relative intensity
Boron B^0	1.1503 (15°K)	(a)	0			∼0.005
Boron B_2^0	1.1319 (15°K)	(a)	18.4			0.05
Boron B^{TO}	1.0924 (15°K)	(a)	57.9			1.00
Boron B_3^{TO}	1.067 (30°K)			(c)	∼38	
Boron B_4^{TO}	1.0599 (15°K)			(a)	32.5	0.025
Boron B_5^{TO}	1.0279 (15°K)			(a)	64.5	0.05
Gallium Ga^0	1.1492 (30°K)	(a)	0			0.30
Gallium Ga_2^0	1.1313 (30°K)	(a)	17.9			0.07
Gallium Ga_7^0	1.074 (80°K)	(c)	87			
Galleum Ga^{TO}	1.0914 (30°K)	(a)	57.8			1.00
Gallium Ga_3^{TO}	1.0364 (30°K)			(c)	68.4	
Gallium Ga_5^{TO}	1.0285 (30°K)			(a)	∼63	∼0.02
Indium In^0	1.1413 (30°K)	(a)	0			3.8
Indium In_3^0	1.008 (100°K)	(c)	151			
Indium In^{TO}	1.0835 (30°K)	(a)	57.8			
Indium In_3^{TO}	∼0.950 (100°K)			(c)	∼150	
Aluminum Al^0	1.1494 (30°K)	(a)	0			0.25
Aluminum Al_2^0	1.1310 (30°K)	(a)	18.4			0.09
Aluminum Al^{TO}	∼1.092 (30°K)	(a)	∼57.5			1.00

[a] The notation is the same as Table II. The following values of exciton energy gap were assumed: 1.1553 eV (15°K); 1.1548 eV (∼30°K); 1.1523 eV (80°K); and 1.1503 eV (100°K).

are therefore artifacts of the apparatus. It is believed they are due to scattered exciting radiation from the mercury lamp comprising green and infrared light recorded, respectively, in second- and first-order diffraction from the grating. These instrumental bands were only observed in high-gain spectra recorded with wide spectrometer slits.

(4) Aluminum

Figure 11 contains relatively weak extrinsic bands due to excitons bound to neutral aluminum acceptors. Only the Al_2^0 and Al^{TO} satellite lines can be identified (Table III).

IV. IDENTIFICATION OF TRANSITIONS RESPONSIBLE FOR THE EXTRINSIC LUMINESCENCE BANDS

A. Phonon Replicas of Bound-Exciton Transitions

The principal bound-exciton satellite in the silicon luminescence spectra, at ∼58 meV below the no-phonon line, has been identified with the TO(MC) phonon replica.[5] This assignment has already been used in the construction of Tables II and III. Comparison of these tables shows that the weaker satellites $(_2^0)$ and $(_5^{TO})$ are, respectively, displaced below the BE no-phonon line and TO(MC) phonon replica by 18.3±0.2 and 64.5±0.2 meV, independent of the nature of the donor or acceptor center. These energies are identical with those of the TA(MC) and O^Γ phonons of the pure lattice deduced from Table I. The $(_2^0)$ and $(_5^{TO})$ BE satellites may therefore also be attributed to electronic transitions involving these two phonons.

Tables II and III show that the intensities of the $(_2^0)$ satellites are ∼5% of the TO(MC) satellite intensity, also independent of the donor or acceptor center except for a slight tendency for this relative intensity to increase in spectra involving the more tightly bound exciton states. The corresponding intensity ratio in the intrinsic spectrum (Table I) is significantly less (3.5%). Precisely the same value of this ratio might be expected for the intrinsic and extrinsic components for sufficiently shallow bound exciton states, since these transitions are closely related to the intrinsic recombinations of free excitons as evidenced by the extent to which the MC phonon replicas predominate in the bound-exciton spectra. The disagreement between the relative intensities of the $(_5^{TO})$ satellites in the bound-exciton spectra (∼2% of the principal TO satellite) and the corresponding intrinsic components (∼7% of the TO replica) is even more pronounced. The excess breadth of the I^{TO+O^Γ} component compared with I^{TO} (Fig. 1) indicates that there is appreciable coupling to phonon pairs with lower total energy than $TO(MC)+O^\Gamma$ in the free-exciton transitions, whereas this does not occur in the bound-exciton recombinations. Momentum conservation may occur in the free-exciton transitions by the emission of two phonons with noncollinear wave vectors. These additional transitions are presumably responsible for the greater relative strength of the intrinsic two-phonon component.

It is interesting that the intensities of the TO(MC) and $TO(MC)+O^\Gamma$ replicas are closely related for all these different impurity centers. The probability of a *single* O^Γ phonon-assisted transition is expected to be
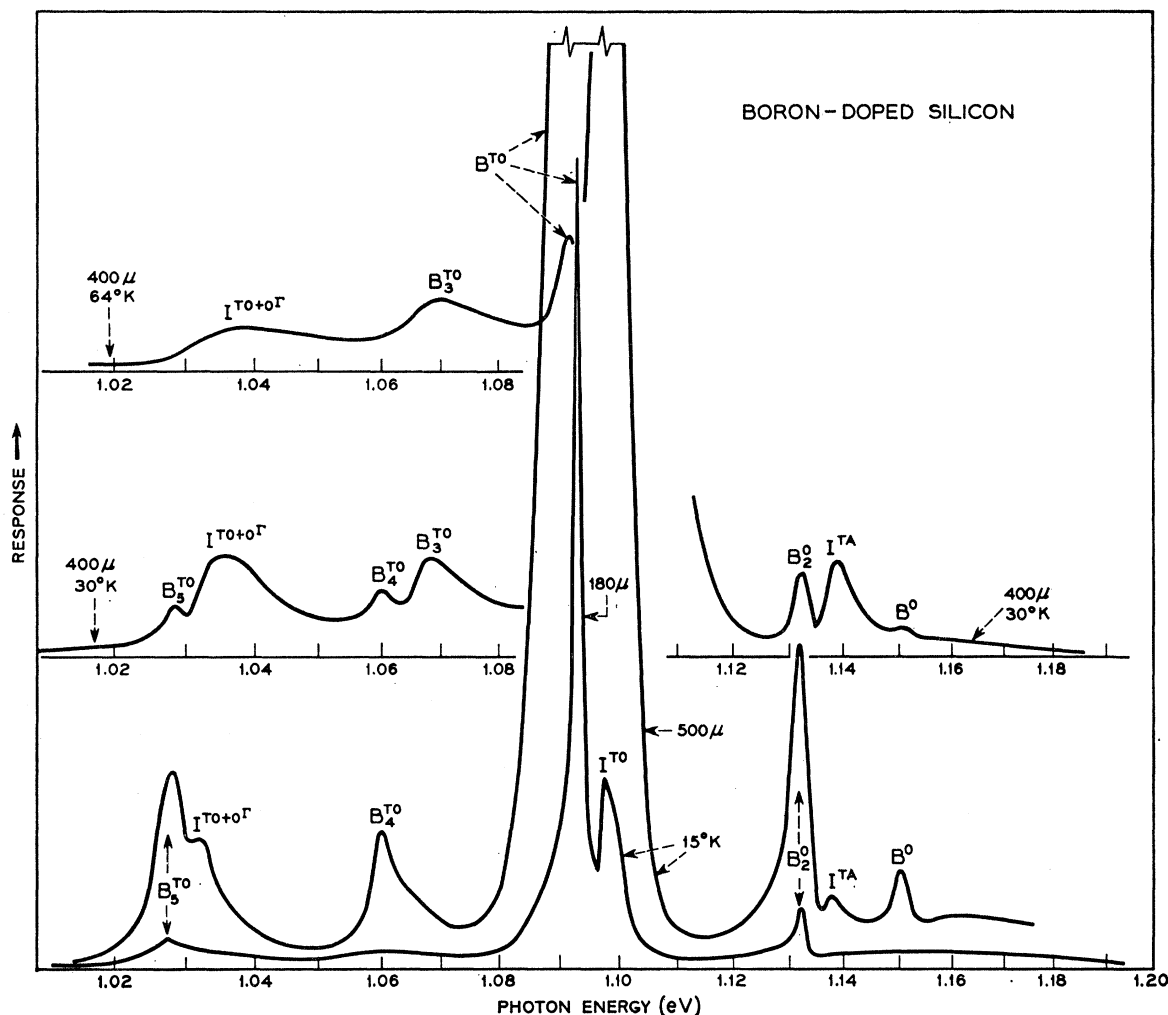
FIG. 8. Photoluminescence spectra from a silicon crystal containing 6×10^{16} cm^{-3} boron atoms. Components B are extrinsic, components I are intrinsic. The notation is consistent with Figs. 2 and 3, and is discussed in the text. The ordinate is nearly proportional to the number of photons per unit energy interval.

closely related to that of the no-phonon transition. This has recently been verified in the luminescence of excitons bound to different neutral donor centers in gallium phosphide.[17] The no-phonon transitions are generally much weaker relative to the MC phonon-assisted transitions for silicon, however, and the single O$^\Gamma$-phonon replica was not detected.

The relative strength of the no-phonon transition for this complex in silicon increases rapidly with the localization energy of the exciton at the impurity

TABLE IV. Analysis of two-electron transitions for excitons bound to neutral donors.

Donor and component	Observed displacement energy (meV)[a]	Corresponding donor transition and energy (meV)	
Arsenic As$_4^0$, As$_4^{TO}$	42.3±0.3	$(1s \rightarrow 2p_0)$, 42.2[b];	$[1s \rightarrow 2s(A_1)]$, 42.6±1.5[c]
Phosphorus P$_4^0$, P$_4^{TO}$	33.6±0.3	$(1s \rightarrow 2p_0)$, 34.1;	$[1s \rightarrow 2s(A_1)]$, 34.8±1.5
Antimony Sb$_4^0$, Sb$_4^{TO}$	31±0.5	$(1s \rightarrow 2p_0)$, 31;	$[1s \rightarrow 2s(A_1)]$, 31.9±1.5

[a] Taken from Table II.
[b] Transition energies of experimentally observed infrared absorption bands (Ref. 20).
[c] Calculated from the experimentally observed transition energies of infrared absorption bands using the corrected theoretical values of the energy separations of the $2p_0$ and $2s(A_1)$ excited states (Ref. 21).

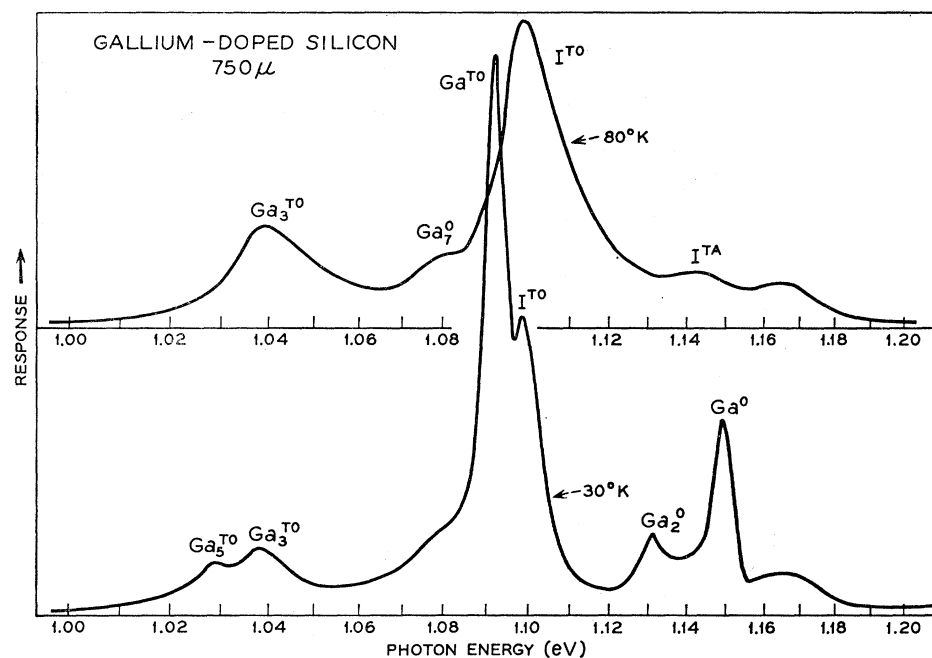[17] P. J. Dean, Phys. Rev. **157**, 655 (1967).

FIG. 9. Photoluminescence spectra from a silicon crystal containing 1.5 $\times 10^{17}$ cm^{-3} gallium atoms. Components Ga are extrinsic, components I are intrinsic. The notation is consistent with Figs. 2 and 3, and is discussed in the text. The ordinate is nearly proportional to the number of photons per unit energy interval.

center (Fig. 12). This increase can be qualitatively understood, since momentum conservation for a no-phonon indirect transition takes place through the coupling between the exciton and the immobile impurity center. The strength of this coupling has been shown to be proportional to the ionization energy of these centers in silicon.[5]

The presence in Fig. 12 of a threshold exciton localization energy, below which a bound-exciton transition apparently does not occur, is less easily understood. According to the simple theory, excitons are expected to bind to neutral donors and acceptors under all possible circumstances of impurity-center ionization energy and reduced mass of the charge carriers.[18]

It is curious that the only ($_5^{TO}$) replica which shows a deviant (large) intensity relative to the principal BE TO(MC) replica is that for boron (Table III), even though the relative intensity of the boron no-phonon line is the lowest observed.

B. "Two-Electron" Transitions Involving Bound Excitons in Silicon

(1) Donor Centers

"Two-electron" transitions, in which the donor electron is either left in an excited bound state or is ejected into the conduction band, have recently been observed in the low-temperature photoluminescence of excitons bound to shallow donor centers in gallium phosphide.[6] Table IV shows that the energy displacements of silicon satellites ($_4^0$) and ($_4^{TO}$) given in Table

II are roughly consistent with a similar identification according to a comparison with the known $1s \rightarrow 2p_0$ interbound state transition energies of donors in silicon.

If the infrared-active $1s \rightarrow 2p$-type excitations were produced in these "two-electron" transitions, as is so for bound excitons in gallium phosphide,[6] the strong $1s \rightarrow 2p_\pm$ transitions would be expected to predominate in the spectra. The $1s \rightarrow 2p_\pm$ transition energies are ~ 5 meV larger than $1s \rightarrow 2p_0$ for donors in silicon,[19] and are definitely inconsistent with the observed displacement energies given in column 2 of Table IV.[20,21] We therefore conclude that the donor transition relevant to these "two-electron" components is $1s \rightarrow 2s$-like, which cannot be observed in the infrared absorption spectra. This conclusion is consistent with the observation of "two-electron" luminescence components involving transitions between $1s$ donor states split by valley-orbit coupling (Sec. IV C), which are also forbidden for a one-photon absorption process.

The intensities of these two-electron components in silicon amount to ~ 3 to 5% of the intensity of the principal bound-exciton components, approximately independent of whether the transition is no-phonon or phonon-assisted. A very similar integrated strength of

[18] J. J. Hopfield, in *Proceedings of the International Conference on Semiconductor Physics, Paris, 1964* (Dunod Cie., Paris, 1964), p. 725.

[19] W. Kohn, in *Solid State Physics*, edited by F. Seitz and D. Turnbull (Academic Press Inc., New York, 1957), Vol. 5, p. 257.
[20] J. W. Bichard and J. C. Giles, Can. J. Phys. **40**, 1480 (1962).
[21] W. Kohn and J. M. Luttinger, Phys. Rev. **98**, 915 (1957). Note that the accuracy of the $1s \rightarrow 2s(A_1)$ transition energies in column 4 of Table IV is limited mainly by uncertainties in these theoretical estimates of the $2p_0 \rightarrow 2s(A_1)$ energy intervals. The $2s(E+T_1)$ excited states are calculated to be 0.5 to 1.6 meV above $2s(A_1)$, depending on the donor. Two-electron transitions involving this state are therefore insignificant according to the displacement energies listed in column 2 of Table IV.
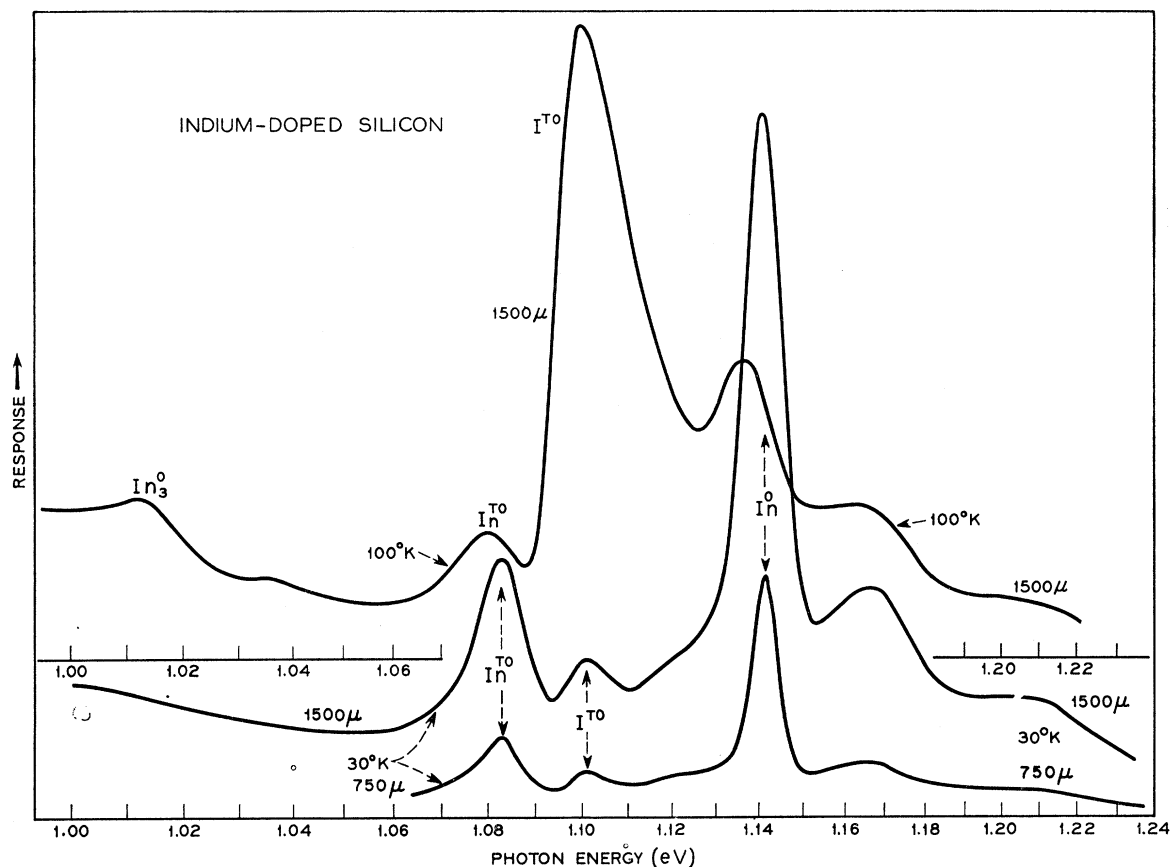
FIG. 10. Photoluminescence spectra from a silicon crystal containing 1.5×10^{16} cm^{-3} indium atoms. Components In are extrinsic, components I are intrinsic. The notation is consistent with Figs. 2 and 3, and is discussed in the text. The ordinate is nearly proportional to the number of photons per unit energy interval.

the discrete two-electron lines was observed for donors in gallium phosphide,[6] although the totally radiationless (Auger) decay rate is $\sim 10 \times$ stronger for donors in silicon.[8] This supports the view that different transition mechanisms are responsible for the Auger and two-electron recombination processes.

The detectability of these components was such that the expected additional satellites corresponding to interbound state transitions involving higher s-like donor excited states, and the two-electron luminescence continuum resulting from ionization of the donor,[6] would not have been observed in these experiments if they are significantly weaker than the $1s \to 2s$ components, as is likely. This remark also applies to the

other two-electron luminescence satellites involving $1s \to 2s$ transitions discussed below.

(2) Acceptor Centers

Bound-exciton satellite B_4^{TO} (Fig. 8) is displaced below the principal TO(MC) replica by an energy midway between the two lowest-energy bands in the interbound state absorption spectrum of boron acceptors in silicon.[22] It is most probable that, as for the donors discussed above, the acceptor two-electron transitions involve hole excitations which are forbidden in the one-photon absorption process (Table V).

C. Two-Electron Transitions Involving Free Excitons and Valley-Orbit States of Donors in Silicon

Satellite transitions $(_1{}^0)$ and $(_1{}^{TO})$ are spaced below the principal BE components by energies significantly less than the known minimum separations between valley-orbit states $1s(A_1)$ and $1s(T_1)$ for donors in

TABLE V. Analysis of two-electron transitions for excitons bound to neutral acceptors in silicon.

Acceptor and component	Observed displacement energy (meV)[a]	Corresponding acceptor transition and energy (meV)[b]
Boron B_4^{TO}	32.5 ± 0.3	$(1 \to 2)30.2$; $(1 \to 3)34.5$

[a] Taken from Table III.
[b] Energies of experimentally observed infrared absorption bands (Ref 22).

[22] J. J. Hrostowski and R. H. Kaiser, Phys. Chem. Solids **4**, 148 (1958).
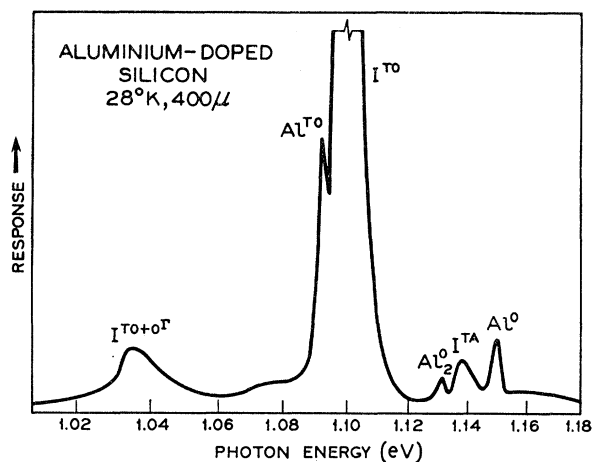[23] R. L. Aggarwal, Solid State Commun. **2**, 163 (1964).

FIG. 11. Low-temperature photoluminescence spectrum from a silicon crystal containing 2×10^{16} cm^{-3} aluminum atoms. Components Al are extrinsic, components I are intrinsic. The notation is consistent with Figs. 2 and 3, and is discussed in the text. The ordinate is nearly proportional to the number of photons per unit energy interval.

silicon,[23] as is clearly seen from Figs. 4 and 5. This fact and the experimental observation that these components are related in intensity to the free-exciton bands rather than to the principal bound-exciton components, and can be seen to have Maxwell-Boltzmann intensity profiles (Sec. III B), leads to the view that the relevant two-electron transitions at temperatures $\gtrsim 64°$K involve *free* excitons in the vicinity of neutral donor centers. When the $(_1{}^0)$ component is relatively strong, then TA(MC) as well as TO(MC) replicas can be detected. This is the origin of component $P_6{}^0$, 18.4 meV below $P_1{}^0$ (Table II). Note that $Sb_6{}^0$ can be observed in Fig. 5, even though $Sb_1{}^0$ is too weak to be detected.
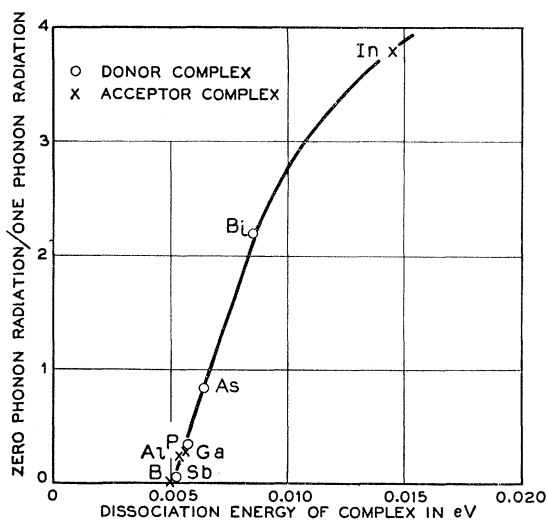

FIG. 12. The intensity ratio of the no-phonon and principal TO(MC) phonon-assisted luminescence bands for excitons bound to neutral donor and acceptor centers in silicon as a function of the localization energy of the exciton in the complex.

The displacement energies appropriate to this model (Tables II and III) are compared in Table VI with the valley-orbit splittings of the 1s-like ground state for three donors. Good agreement is obtained for all three donors if it is assumed that the $1s(A_1) \rightarrow 1s(E)$ transition is dominant in the two-electron spectra.[24] Agreement with experiment is poor using other models for these components, such as the recombination of free-electron–hole pairs at neutral donors. Since these components are prominent at low temperature (Sec. III A), where the majority of the excess carriers are in free-exciton states,[3] it is in any event most probable that they involve recombination of excitons rather than free-electron hole pairs. This recombination process remains prominent at least up to 80°K, when the bound-exciton transitions are insignificant.[5]

Because of thermalization, essentially all of the donors are in the $1s(A_1)$ ground state at $\lesssim 30°$K. This is still by far the most heavily populated bound state at 80°K, even for antimony which has the smallest valley-orbit energy splittings (Table VI). The existence of the free-exciton two-electron transition depends upon the fact that the donor wave function becomes distorted through interaction with a nearby free exciton, and contains components from the higher-energy valley-orbit states. The matrix element for this recombination process is expected to be large only when the energy separation of the relevant valley-orbit states does not greatly exceed the internal binding energy of the free exciton. The experimental observation that the free-exciton two-electron transitions are relatively prominent in the low-temperature luminescence spectra for phosphorus and antimony donors (Figs. 4–6), which have small valley-orbit energy separations compared with arsenic and bismuth donors (Figs. 2, 3, and 7), is therefore readily understood.

The general strength of these two-electron transitions in which the valley-orbit state of the donor changes remains a problem. Free-exciton recombinations involving no change in the energy state of the donor might be anticipated to occur in significant proportion P to those analyzed in Table VI. The recombination process could involve transitions for which $P \ll 1$, for example, if the donor electron recombines with the hole of the free exciton leaving the wave function of the electron from the exciton distributed amongst the valley-orbit sub-levels of the 1s-like donor ground state. If the initially uniform distribution of the electron wave function in the free exciton amongst the six conduction-band valleys is preserved in the transition, then $P = \frac{1}{6}$. This prediction can only be

[24] A transition between the $1s(A_1)$ and $1s(E)$ valley-orbit states has recently been identified in Raman scattering from phosphorus donors in silicon [G. B. Wright and A. Mooradian, Phys. Rev. Letters 18, 608 (1967)]. Although the $1s(A_1) \rightarrow 1s(T_2)$ transition is symmetry allowed, detailed considerations of the donor wave functions show that the strength of this transition is zero unless interactions with p-like higher-energy states are included.

TABLE VI. Analysis of two-electron transitions for free excitons interacting with neutral donors in silicon.

Donor and component	Observed displacement energy (meV)[a]	Corresponding donor transition and energy (meV)[b]
Arsenic As_1^0, As_1^{TO}	22.3 ± 0.5	$[1s(A_1) \rightarrow 1s(T_1)]21.2$; $[1s(A_1) \rightarrow 1s(E)]22.6$
Phosphorus P_1^0, P_1^{TO}	13.5 ± 0.3	$[1s(A_1) \rightarrow 1s(T_1)]11.9$; $[1s(A_1) \rightarrow 1s(E)]13.2$
Antimony Sb_1^{TO}	12.1 ± 0.3	$[1s(A_1) \rightarrow 1s(T_1)]9.9$; $[1s(A_1) \rightarrow 1s(E)]12.4$

[a] Taken from Table II.   [b] Deduced from infrared absorption spectra (Ref. 23).

tested for the no-phonon recombinations, since these phonon-assisted donor-induced components occur at the same energies as the intrinsic free-exciton components, and would be masked by them. The no-phonon valley-orbit two-electron components are sufficiently strong for this prediction to be tested only for phosphorus donors and it is estimated from Fig. 4 that $P \lesssim 1/30$. We must therefore assume that the strength of the two-electron transitions in which the donor is left in the $1s(A_1)$ singlet state is limited by a selection rule.

The apparent increase in half-width of these components as the temperature is *reduced* below 20.6°K (e.g., Fig. 5) may be due to the superposition at the lower temperatures of displaced but unresolved *bound-exciton* two-electron components involving valley-orbit donor transitions.[25] An additional weak component (20% of P^0) was resolved on the low-energy tail of P_1^0 in one specimen containing a lower concentration of phosphorus, instead of the broad tail shown in Fig. 4. This band was 13.5 meV below component P^0, consistent with expectation for *bound-exciton* two-electron transitions involving excitations between valley-orbit states of the phosphorus donor (Table VI). Corresponding TA and TO phonon-assisted transitions were also observed. This additional structure is easier to see at 21°K than at 15°K because of enhanced low-energy tailing observed at the lower temperature for all these components.

The reduced half-width (compared with the M.B. profile) of the $(_1^0)$ and $(_1^{TO})$ components mentioned in Section III B presumably results from a reduction in the interaction cross section for the two-electron process with the velocity of the free exciton. It was not possible to obtain a reliable quantitative estimate of this velocity dependence.

No transitions of comparably small displacement energy relative to the ionization energy of the impurity center were observed in the luminescence of excitons bound to neutral acceptor centers. This is consistent with the above model, since there are no valley-orbit states for acceptors in silicon.

[25] Recent measurements of free-exciton transitions in silicon by the present authors have revealed a weak absorption component ~ 1.7 meV below the previously recognized value of E_{gx} (see Ref. 3) which has been used in the present paper. This lower-energy free-exciton state becomes significantly populated below ~ 20°K. Two-electron valley-orbit transitions induced by the recombination of these lower-energy free excitons may also contribute to the broadening of component Sb_1^{TO} as the temperature is reduced (Fig. 5).

D. Two-Electron Recombinations Involving the H^--Like Complex as an Intermediate State

(1) Donor Centers

The remaining extrinsic luminescence bands associated with the presence of neutral donors in silicon, $(_3^0)$ and $(_3^{TO})$, were only observed at intermediate or higher temperatures in the investigated range 15°K $\rightarrow \sim 80$°K (e.g., Figs. 2, 4, and 8) in contrast to the bound-exciton components (Sec. IV B). This implies that components $(_3^0)$ and $(_3^{TO})$ involve free carriers rather than free excitons.[10] The $(_3^{TO})$ components shown in Figs. 2–4 are well approximated by M.B. intensity profiles broadened by the effect of the finite spectral resolution, implying that there is only one free particle in the initial state of the luminescence transition.[3] Thus, a possible recombination process might be the radiative capture of free holes at neutral donors, a process which has already been reported in silicon.[26] Table VII shows that the observed displacement energies are ~ 7-meV smaller than would be expected on the basis of this model (model I), however, but are consistent with a more complicated mechanism (model II) involving two distinct capture processes.

(a) Capture of a free electron by a neutral donor to form the weakly bound H^--like donor complex originally conceived by Lampert.[7]

(b) Radiative capture of a free hole by the H^--like donor complex, leaving the donor electron in an excited state.

This mechanism is consistent with the experimental observation that, at 64°K, the intensities of components $(_3^{TO})$ vary as the *square* of the excitation intensity, as do components $(_1^{TO})$ and the principal free-exciton component I^{TO}. This is the expected result for the recombination of either excess electrons and holes or excitons, since few excess carriers are bound as excitons at 64°K. For constant carrier lifetime the exciton concentration n_x is proportional to product np of the concentrations of excess electrons and holes.

The donor excitation involved in these two-electron recombinations must be either $1s \rightarrow 2p_0$ or $1s \rightarrow 2s$ if the desired positive value of the binding energy of the second electron in the H^--like donor complex is to be obtained. The arguments of Sec. IV B may be again

[26] Ya. E. Pokrovskii and K. I. Svistunova, Fiz. Tver. Tela **5**, 1880 (1963); **6**, 19 (1964) [English transls.: Soviet Phys.—Solid State **5**, 1373 (1963); **6**, 13 (1964)].

TABLE VII. Analysis of two-electron transitions involving the radiative recombination of free
holes at negatively charged (H⁻-like) donors in silicon.

Donor and component	Observed displacement energy (meV)	Calculated displacement energy (meV)—free holes at neutral donors (model I)[a]	Calculated displacement energy (meV)—free holes at H⁻-like complex involving two-electron transition (model II)[b]		
Arsenic As_3^0, As_3^{TO}	47.5±0.5	53.5	47.5 if	$E_s=10.9$	and $E_T=4.9$
Phosphorus P_3^{TO}	38.5±0.5	45.3	38.5 if	$E_s=10.5$	and $E_T=3.7$
Antimony Sb_3^{TO}	36.0±1.0	43	36.0 if	$E_s=9.3$	and $E_T=3.3$

[a] Calculated assuming that the observed M.B. threshold transition energy is given by $h\nu=E_g-E_D$, where E_D is the donor ionization energy.
[b] Calculated assuming that the observed M.B. threshold transition energy is given by $h\nu=E_g-E_D+(E_s-E_T)$, where E_s is the binding energy of the 2s donor excited state, and E_T is the binding energy of the second electron at the neutral donor (see text).

used to show that the $1s \rightarrow 2p_0$ assignment is unlikely. The theoretical binding energy of the $2s(A_1)$ state[21] has been used for E_s in Table VII, consistent with the assignments in Sec. IV B. The resulting values of E_T in Table VII are subject to an uncertainty of $\sim\pm1.5$ meV because of uncertainties in the theoretical values of E_s for the $1s(A_1)$ states.[21]

An estimate for E_T may also be obtained from measurements of the temperature-dependent ratio R of the ($_1^{TO}$) and ($_3^{TO}$) component intensities. It is easy to show that for temperatures T_1 and T_2, assuming the models proposed in this section and in Sec. IV C,

$$\frac{R_{T_1}}{R_{T_2}} = \exp\left[\frac{(E_x-E_T)}{kT_1} - \frac{(E_x-E_T)}{kT_2}\right], \quad (1)$$

where k is Boltzmann's constant.

Data from the arsenic-doped crystal shown in Figs. 2 and 3 gave $R_{29}/R_{64}=3\pm1$, so that $E_x-E_T=5\pm1$ meV according to Eq. (1). If $E_x=8$ meV,[3] this implies that $E_T\sim3\pm1$ meV. This estimate is consistent with those given in Table VII, considering the large uncertainties involved. The relationship $E_T=0.055\times E_D$, obtained from the analogy with the H⁻ ion,[7] gives $E_T=1.6$ meV if the effective-mass value $E_D=29$ meV[20] is used for donors in silicon, as seems reasonable considering the small value of the ratio E_T/E_D.

Comparison of Figs. 2 and 3 shows that the As_3^{TO} component has a low-energy tail which is more prominent at higher temperatures. The extent of this tail suggests that it may arise from the radiative recombination of free holes at neutral arsenic donors. This model-I transition (Table VII) might be expected to be more important at 64°K than at 29°K in view of the small value of E_T deduced above, but Fig. 3 shows that the majority of the luminescence still results from the two-electron transition even at 64°K. This is to be contrasted with the mechanisms of the comparable transitions for the deeper acceptor centers in silicon discussed in the next section.

(2) Acceptor Centers

Table VIII shows that the boron component B_3^{TO}, which has an M.B. intensity profile, may be interpreted in terms of a two-electron transition very similar to the donor transitions just discussed. The relevant acceptor excitation is assumed in Table VIII to be the lowest-energy strong transition, energy 34.5 meV, observed in the infrared absorption spectra.[22] A rather large value, ~5.5 meV, is derived for E_T if the 32.5-meV excitation energy deduced from the bound-exciton two-electron transition for boron (Sec. IV B) is used.

The displacement energies of the ($_3^{TO}$) components observed in the gallium and indium spectra are, by contrast, much closer to those predicted for the recombination of free electrons at neutral acceptors (model I) rather than for the two-electron (model II) transition, within the limits imposed by the rather poor resolution in these spectra (Figs. 9 and 10). The model-II transition is only possible for these acceptors if the hole is in a very high excited state after the recombination process, which seems unlikely in view of the nature of the other two-electron transitions observed for other donors and acceptors in silicon.

TABLE VIII. Analysis of transitions involving the radiative recombination of free electrons at acceptor complexes in silicon.

Acceptor and component	Observed displacement energy (meV)	Calculated displacement energy (meV)—free electrons at neutral acceptors (model I)[a]	Calculated displacement energy (meV)—free holes at H⁻-like complexes (model II)[b]	
Boron B_3^{TO}	38 ±0.5	46	38 if $E_s=11.5$	and $E_T=3.5$
Gallium Ga_3^{TO}	68.4±1.5	71	Not possible	
Indium In_3^0	150 ±3	154	Not possible	

[a] Calculated assuming that the observed M.B. threshold transition energy is given by $h\nu=E_g-E_A$, where E_A is the acceptor ionization energy.
[b] Calculated assuming that the observed M.B. threshold transition energy is given by $h\nu=E_g-E_A+(E_s-E_T)$, where E_s corresponds to the strong $1 \rightarrow 3$ infrared absorption band (Ref. 22).

In agreement with these conclusions, Pokrovskii and Svistunova have reported photoluminescence due to the recombination of free electrons at neutral gallium and indium acceptors in silicon.[26] They also observed that the principal extrinsic luminescence component for gallium involved the TO(MC) phonon, whereas the no-phonon component was predominant for transitions at the very deep indium acceptor, in agreement with Figs. 9 and 10. Component $Ga_7{}^0$, also shown in Fig. 9, is the TA(MC) replica of $Ga_3{}^0$, and is thus TO(MC) −TA(MC) or ∼39 meV above the prominent component $Ga_3{}^{TO}$ (Table III). The present results are in sharp disagreement with the conclusion of Pokrovskii and Svistunova that the model-I recombination mechanism is predominant in the low-temperature photoluminescence spectra of boron-doped silicon, however. This disagreement may stem from differences in the type of doping employed in the two investigations. Silicon single crystals used in the present work were chemically very pure except for the particular donor or acceptor under investigation. Pokrovskii and Svistunova used specially double doped crystals. For example, recombination at boron acceptors was measured in the presence of excess antimony donors to provide a source of free electrons additional to interband photoexcitation

Photoluminescence spectra obtained from boron and phosphorus double-doped silicon by the present authors exhibited structure consistent with Figs. 4 and 8, however, except that donor-acceptor pair transitions (see Sec. IV E) were also observed. Weak additional boron bound-exciton components were observed under excitation in the n-type region of the crystal, also phosphorus BE components under p-region excitation. This is possible because many of the compensated centers become neutralized under continuous high-intensity interband excitation at low temperatures.

Careful examination of the spectral position and other properties of the observed luminescence bands has shown that the radiative recombination of free holes at neutral arsenic, phosphorus, and antimony donors in silicon is *not* a dominant process at least in the temperature range investigated here ($\lesssim 80°$K). Pokrovskii and Svistunova claim that the model-I transition is predominant in the photoluminescence of bismuth-doped silicon, however.[26] The relevant components were not detected in the present work (Fig. 7). It is plausible to assume that model-I transitions may be relatively more important for a donor like bismuth, which has a large ionization energy, in view of the trend shown in Table VIII for acceptor centers.

E. Luminescence Due to Donor-Acceptor Pair Recombinations

It is important to be sure that none of the luminescence bands discussed in this paper arise from interimpurity recombinations of electrons and holes,

respectively bound to donor and acceptor centers. Donor-acceptor pair bands have been observed by the present authors only in luminescence from deliberately compensated silicon. The donor-acceptor pair bands in silicon are very broad and featureless[27] and are therefore easily distinguished in the low-temperature spectra from the spectrally well-defined extrinsic components discussed above. They are relatively weak compared with the exciton luminescence under high-intensity excitation even at compensation levels ∼10^{16} cm^{-3}. The crystals used in the work reported in this paper were very pure except for the single desired dopant, and the luminescence was always recorded under high-intensity excitation. Donor-acceptor pair transitions are known to be negligible for silicon under these conditions.[28]

V. TWO-ELECTRON LUMINESCENCE TRANSITIONS IN GERMANIUM

There are several unidentified lines in the detailed edge photoluminescence spectra of doped germanium reported by Benoit à la Guillaume and Parodi[29] (hereafter called G.P.). It is natural to seek an interpretation of this structure in terms of the various two-electron transitions discussed above for silicon.

A. Two-Electron Transitions Involving Valley-Orbit Donor Excitations

Two closely spaced and relatively sharp lines observed by G.P. only for the donors phosphorus and arsenic (labeled B and C in order of increasing transition energy) were attributed to the recombination of excitons at these neutral donors. The presence of two such components cannot be explained by spin-spin interactions, since the two electrons in this exciton-impurity complex should simply pair off in an antisymmetric state.[30] It is noticeable in the spectra for phosphorus donors reported by G.P. that component B is generally broader than C and becomes more prominent relative to C with increasing temperature. This behavior is very similar to that reported for the silicon satellites ($_1{}^0$) and ($_1{}^{TO}$) above (Sec. IV C), and suggests that the germanium B components may also arise from two-electron transitions in which a free exciton recombines near a donor center and the donor electron is excited between valley-orbit states derived from the 1s-like hydrogenic ground state. This suggestion is further supported by the agreement between columns

[27] A. Honig and R. Enck, in *Proceedings of the International Symposium on Radiative Recombination, Paris, 1964* (Dunod Cie., Paris, 1964), p. 113.

[28] Ya. E. Pokrovskii and K. I. Svistunova, Fiz. Tver. Tela **7**, 1837 (1965) [English transl.: Soviet Phys.—Solid State **7**, 1478 (1965)].

[29] C. Benoit à la Guillaume and O. Parodi, in *Proceedings of the International Conference on Semiconductor Physics, 1960* (Czechoslovakian Academy of Sciences, Prague, 1961), p. 426.

[30] D. G. Thomas and J. J. Hopfield, Phys. Rev. **128**, 2135 (1962).

TABLE IX. Analysis of two-electron transitions for free excitons interacting with neutral donors in germanium.

Donor and component	Energy relative to C (meV)[a]	Energy relative to E_{gx} (meV)[a]	Corresponding donor transition $[1s(A_1)-1s(T_1)]$ and energy (meV)[b]
Arsenic, B	2.4	4.3±0.2	4.23±0.02
Phosphorus, B	1.5 (4 and 14°K)	3.1±0.2	2.83±0.02
Antimony, B	~0? (B and C not resolved)	~1	0.32±0.02

[a] From the luminescence spectra of Ref. 29, assuming that E_{gx} is 0.7405 eV for germanium at $T \lesssim 14°$K.
[b] From optical absorption data of Ref. 31.

3 and 4 in the analysis of transition energies given in Table IX.[31] The fraction P of these two-electron transitions which leave the donor electron in the lowest-energy $1s(A_1)$ valley-orbit state is significantly lower than the value $\frac{1}{4}$ predicted in the absence of selection rules (Sec. IV C). Like silicon, the corresponding two-electron component at E_{gx} was not detected for germanium.

In terms of the present interpretation the labeling arbitrarily used by G.P.[29] should be revised. The single sharp component observed for the acceptors gallium and indium should be labeled C rather than B, since C is the bound-exciton transition and the valley-orbit two-electron component B cannot occur in acceptor spectra. The valley-orbit splitting for the donor antimony is very small in germanium and lines B and C are predicted to be nearly coincident (Table IX), consistent with the experimental observation of only one such line.

Component B is relatively sharp at 14°K in the phosphorus spectra[29] compared with the free-exciton bands, presumably due to the velocity-dependent interaction cross section discussed in Sec. IV C in connection with similar effects observed for corresponding transitions in silicon. At 4.2°K, component B is broader than at 14°K, as observed for the $(_1{}^0)$ and $(_1{}^{TO})$ silicon components (Secs. III B and IV C) but at higher temperatures consistent with the larger ionization energies of the exciton states in silicon. At the same temperature relative to the internal ionization energy of the exciton, E_x, the intensity ratio of the phosphorus B and C components is comparable with that of the corresponding components in silicon. This is consistent with the discussion of Sec. IV C, since the valley-orbit splitting energy of this donor is comparable with E_x in both crystals.

B. Other Two-Electron Transitions in Germanium

Relatively broad bands (A components) at slightly lower energies than components B and C were attributed by G.P.[29] to the radiative recombination of free electrons (or holes) at the various neutral acceptor (or donor) centers studied. The transition energies of the A components vary with the donor and acceptor

ionization energies, as expected from this identification, but are uniformly higher by ~1.4 meV than the calculated values if the exciton binding energy is 3 meV.[32]

It is quite likely that these A components, which are not observed at helium temperatures, involve the radiative recombination of free electrons or holes at the H⁻-like acceptor or donor complexes discussed in Sec. IV D. Then the energy discrepancy of 1.4 meV represents $E_s - E_t$ (Table VII). Since the valley-orbit excitations are prominent in two-electron transitions in germanium, it is likely that the selection rules are such that E_s represents the ionization energy of a $2s$-like excited state as is shown above for silicon. Comparison with theoretical calculations for silicon[21] suggests that E_s may therefore be ~3 meV for donors in germanium, and possibly quite similar for acceptors also. Thus E_t is predicted to be ~1.5 meV, a plausible value although once again appreciably larger than predicted by the relationship $E_t = 0.055 \times E_D$ introduced in Sec. IV D.

The bound-exciton two-electron transitions discussed in Sec. IV B should also occur in donor and acceptor spectra in germanium. An unidentified weak line in the 4.2°K spectrum from a phosphorus-doped crystal reported by G.P.[29] occurs at 0.7293 eV, close to the calculated value for a bound-exciton recombination involving a two-electron transition to a phosphorus excited state of binding energy ~3 meV. This component has intensity comparable to the TA phonon replica of the exciton resonance transition, roughly as observed for phosphorus in silicon (components $P_2{}^0$ and $P_4{}^0$ in Fig. 4).

VI. SUMMARY

The following extrinsic recombination processes have been identified in the low-temperature photoluminescence of *silicon* doped separately with a variety of donor and acceptor centers, in addition to the previously reported no-phonon and TO(MC) phonon-assisted decay of excitions bound to neutral donors and acceptors [BE transitions, components $(^0)$, $(^{TO})$].

---

[31] J. H. Reuszer and P. Fisher, Phys. Rev. **135**, A1125 (1964).

[32] T. P. McLean and R. Loudon, Phys. Chem. Solids **13**, 1 (1960).

A. Phonon-assisted Bound Exciton Recombinations at Neutral Donors and Acceptors

Additional BE phonon-assisted transitions due to the TA(MC) and [TO(MC)+0] phonons [components $(_2{}^0)$, $(_2{}^{TO})$, and $(_5{}^{TO})$]. The energies of these phonons are very similar to those observed in the intrinsic (free-exciton) luminescence bands. The relative intensities of the phonon replicas in the BE and intrinsic spectra are of the same order, but are not identical, the differences being most pronounced for the impurities with the largest ionization energies.

B. Bound Exciton Two-Electron Recombinations at Neutral Donors and Acceptors

Relatively weak BE satellite bands, whose intensities are of order $\sim 1\%$ of the principal bands, have been identified with processes in which a bound electron and hole recombine and part of the energy thus released is used in raising the second electron (donor complex) or hole (acceptor complex) to an excited bound state, the remainder appearing in the detected electromagnetic radiation [components $(_4{}^0)$, $(_4{}^{TO})$].

C. Free Exciton Two-Electron Recombinations at Neutral Donors and Acceptors

Additional two-electron transitions observed in the donor spectra are apparently due to the recombination of free excitons in the vicinity of the donor centers in which part of the transition energy is used to raise the donor electron into an excited level of the $1s$-like hydrogenic ground state produced by valley-orbit coupling [components $(_1{}^0)$, $(_1{}^{TO})$]. At temperatures $\sim 20°K$ the relative intensity of this two-electron transition decreases rapidly with increasing valley-orbit coupling. This transition is readily detected at $80°K$, unlike the BE transitions. Transitions in which the donor is left in the lowest $[1s(A_1)]$ valley-orbit state are unexpectedly weak.

D. Free Carrier Two-Electron Recombinations Involving H⁻-Like Donor and Acceptor Complexes

Two-electron luminescence transitions have also been observed which involve the recombination of free holes (or electrons) with one electron (or hole) in an H⁻-like donor (or acceptor) complex, part of the energy again being used to raise the second electron (or hole) to an excited bound state [components $(_3{}^0)$, $(_3{}^{TO})$]. The ionization energy of the second carrier in the H⁻-like complex is not accurately determined, and may be dependent upon the donor or acceptor center, but a typical value is 4 ± 1 meV, roughly consistent with expectation according to an analogy with the H⁻ ion. These transitions are negligible at $\sim 20°K$, but relatively strong at $\sim 80°K$, consistent with the participation of free carriers rather than free excitons.

E. Free Carrier Recombinations at Neutral Donors and Acceptors

Significant low-temperature (below $\sim 100°K$) luminescence due to the recombination of free carriers with neutral centers was observed only for the acceptors gallium and indium, which have relatively large ionization energies [components $(_3{}^0)$, $(_3{}^{TO})$]. These luminescence components were also observed only at temperatures $\gtrsim 30°K$. It is possible that this recombination process is also prominent for bismuth donors as reported elsewhere,[26] but neither the luminescence bands corresponding to this recombination process or to two-electron processes were detected for bismuth in the present work.

The low-temperature edge photoluminescence spectra of doped *germanium* reported by Benoit à la Guillaume and Parodi[29] have been shown to contain components which are identifiable with these newly discovered two-electron recombination processes. Spectral components associated with the H⁻-like complex and with valley-orbit donor transitions are especially prominent. Like silicon, two-electron free-exciton transitions in which the donor is left in the lowest valley-orbit state were not observed for germanium. The ionization energy of the second particle in the H⁻-like complex is ~ 1.5 meV for several donors and acceptors in germanium.

The two-electron spectra observed for donors in silicon and germanium appear to involve donor transitions between $1s$- and $2s$-like states [or $1s(A_1)$ and $1s(E)$ or $1s(T_1)$ states], not directly observable in the infrared donor photoexcitation spectra. Thus, although the presence of the substitutional impurity atom destroys the local inversion symmetry of the lattice, these results imply that parity is apparently a good quantum number for these indirect transitions in silicon and germanium. Exactly the opposite conclusion was obtained from the character of two-electron transitions involving BE states in gallium phosphide,[6] where the perfect lattice does not possess inversion symmetry.

The detectivity in the present work was adequate only for the observation of the principal $(1s \rightarrow 2s)$ bound-exciton two-electron components. Comparison with the spectra obtained from gallium phosphide suggests that it will be extremely difficult to detect in silicon or germanium the weak luminescence continuum corresponding to two-electron transitions in which free carriers are produced.